had the opposite effect. Therefore, if homosynaptic LTD and LTP are to operate together to allow activity-dependent modification of the stimulus selectivity of neurons[4], this is not likely to occur concomitantly under behavioural conditions such as those examined here. As HFS is shown here to reverse LTD to pre-LFS in stressed animals, and LFS has been reported to reverse LTP in non-stressed rats[7,8,19], such a role for bidirectional plasticity is possible, but with a dynamic range tightly restricted by behavioural state. □

Methods

Electrode implantation. Male Wistar rats, weighing 200–300 g, had electrodes implanted using previously described techniques[19–21]. The surgery was carried out under pentobarbitone sodium (60 mg kg^{-1}, i.p.) anaesthesia, and core temperature was maintained at 37 ± 0.5 °C. Three stainless-steel screws (1.5 mm diameter) were inserted into the skull through a drill hole without piercing the dura. One served as a ground electrode (7 mm posterior to bregma and 5 mm left of the midline), another acted as an anchor (opposite the ground screw, 7 mm posterior to bregma and 5 mm right of the midline) and the third served as the reference electrode (8 mm anterior to bregma and 1 mm left of the midline). Recording and stimulating electrodes were made by gluing together a pair of twisted Teflon-coated platinum (90%)/iridium (10%) wires (50 μm inner diameter, 75 μm outer diameter). The recording electrode was inserted 3.4 mm posterior to bregma and 2.5 mm right of the midline and the stimulating electrode was inserted 4.2 mm posterior to bregma and 3.8 mm right of the midline. In some animals, a second stimulating electrode was placed in the contralateral hemisphere in order to stimulate the commissural pathway. Lack of paired-pulse interaction with responses evoked in the test pathway was used as a criterion of independence. The optimal placement of the electrodes in the stratum radiatum of the CA1 region of the dorsal hippocampus was determined using electrophysiological criteria and was verified by post mortem examination.

Acclimatization. After surgery animals were housed individually (in home cage) with free access to water and food in an established animal house having a 12 h light/dark cycle and thermoregulated environment. Recording began two weeks later to allow the animals to recover from surgery. Acclimatized group: during this recovery period the rats were put in the brightly lit recording box (34 × 24 × 24 cm) for 1 h at the same time each day and the socket assembly on the animal's head was connected to a preamplifier by a flexible wire. By the end of the first week, there was no evidence of behavioural 'freezing' and the rats became very tame and well used to being handled. Unhandled, recording-naive group: the rats were left undisturbed in their home cage during the two-week recovery period.

Electrophysiology. Test field EPSPs were evoked by stimulating with a square-wave constant current pulse of 0.2 ms duration at a rate of 0.033 Hz. At the beginning of each experiment, input–output curves were generated to determine the maximum field EPSP amplitude. Results were similar if the EPSP slope rather than the EPSP amplitude was measured. During the experiments, the stimulus intensity was set at a level that evoked a field EPSP amplitude of 50–60% of the maximum. LFS consisting of 900 pulses at 3 Hz was applied to induce LTD; LTP was induced by HFS (20 pulses at 200 Hz, repeated 10 times at a 2-s interval). The background EEG (monitored from the hippocampal recording electrode) showed no evidence of seizure activity after the conditioning stimulation. To minimize the possibility that changes in locomotor activity might affect the field EPSP amplitude, recordings were not usually taken for the first 20 min after being placed in the recording box unless otherwise stated. Control experiments showed that placement of either recording-naive animals in a brightly lit unfamiliar recording box (stressed) or recording-acclimatized animals in an unfamiliar dimly lit recording box (non-stressed) was associated with a similar small (<1 °C) transient (<10 min) increase in brain temperature (recorded with a precalibrated type-T thermocouple wire (tip diameter, 0.5 mm; accuracy, 0.05 °C) placed on the surface of the contralateral hippocampus or cortex). Serum corticosterone was determined using HPLC. Levels were raised in stress conditions compared to non-stress conditions (recording-naive/unfamiliar recording box, 18.2 ± 5.3; acclimatized/elevated platform, 40.6 ± 7.3; acclimatized/familiar recording box, 3 ± 0.8; acclimatized/novel recording box, 5.2 ± 1.2; recording-naive/home cage 1 ± 0.3 μg dl^{-1}; $n = 4$ per group). Statistical comparisons between baseline and post-conditioning stimulation values were made using Student's t-test. Values are mean per cent of the baseline field EPSP amplitude ± s.e.m.

Received 3 December 1996; accepted 24 March 1997.

1. Diamond, D. M. *et al.* Exposure to a novel environment interferes with the induction of hippocampal primed burst potentiation. *Psychobiology* **18,** 273–281 (1990).
2. Shors, T. J. *et al.* Inescapable versus escapable shock modulates long-term potentiation in the rat hippocampus. *Science* **244,** 224–226 (1989).
3. Linden, D. J. & Connor, J. A. Long-term synaptic depression. *Annu. Rev. Neurosci.* **18,** 319–357 (1995).
4. Bear, M. F. & Abraham, W. C. Long-term depression in hippocampus. *Annu. Rev. Neurosci.* **19,** 437–462 (1996).
5. Dudek, S. M. & Bear, M. F. Bidirectional long-term modification of synaptic effectiveness in the adult and immature hippocampus. *J. Neurosci.* **13,** 2910–2918 (1993).
6. Errington, M. L. *et al.* Stimulation at 1–5 Hz does not produce long-term depression or depotentiation in the hippocampus of the adult rat *in vivo*. *J. Neurophysiol.* **74,** 1793–1799 (1995).
7. Staubli, U. & Lynch, G. Stable depression of potentiated synaptic responses in the hippocampus with 1–5 Hz stimulation. *Brain Res.* **513,** 113–118 (1990).
8. Doyle, C. A. *et al.* Low-frequency stimulation induces homosynaptic depotentiation but not long-term depression of synaptic transmission in the adult anaesthetized and awake rat hippocampus *in vivo*. *Neuroscience* **77,** 75–85 (1997).
9. Balfour, D. J. K. & Reid, A. Effects of betamethasone on the stimulation of corticosterone secretion in rats. *Arch. Int. Pharmacodyn. Ther.* **237,** 67–74 (1979).
10. Barrionuevo, G., Shottler, F. & Lynch, G. The effects of repetitive low frequency stimulation on control and "potentiated" synaptic responses in the hippocampus. *Life Sci.* **27,** 2385–2391 (1980).
11. Thiels, E., Barrionuevo, G. & Berger, T. W. Excitatory stimulation during postsynaptic inhibition induces long-term depression in hippocampus *in vivo*. *J. Neurophysiol.* **72,** 3009–3016 (1994).
12. Heynen, A. J., Abraham, W. C. & Bear, M. F. Bidirectional modification of CA1 synapses in the adult hippocampus *in vivo*. *Nature* **381,** 163–166 (1996).
13. Joëls, M. & de Kloet, E. R. Corticosteroid hormones: endocrine messengers in the brain. *News Physiol. Sci.* **10,** 71–76 (1995).
14. Diamond, D. M. *et al.* Inverted-U relationship between the level of peripheral corticosterone and the magnitude of hippocampal primed burst potentiation. *Hippocampus* **2,** 421–430 (1992).
15. Kerr, D. S. *et al.* Modulation of hippocampal long-term potentiation and long-term depression by corticosteroid receptor activation. *Psychobiology* **22,** 123–133 (1994).
16. Pavlides, C. *et al.* Hippocampal homosynaptic long-term depression/depotentiation induced by adrenal steroids. *Neuroscience* **68,** 379–385 (1995).
17. Kim, J. J., Foy, M. R. & Thompson, R. F. Behavioral stress modifies hippocampal plasticity through *N*-methyl-D-aspartate receptor activation. *Proc. Natl Acad. Sci. USA* **93,** 4750–4753 (1996).
18. Bear, M. F. Mechanism for a sliding synaptic modification threshold. *Neuron* **15,** 1–4 (1995).
19. Doyle, C. A. *et al.* The selective neuronal NO synthase inhibitor 7-nitro-indazole blocks both long-term potentiation and depotentiation of field EPSPs in rat hippocampal CA1 *in vivo*. *J. Neurosci.* **16,** 418–426 (1996).
20. O'Connor, J. J., Rowan, M. J. & Anwyl, R. Serotonergic involvement in the inhibitory effects of repeated buspirone treatment on synaptic transmission in the hippocampus of alert rats. *Eur. J. Pharmacol.* **167,** 21–29 (1989).
21. Manahan-Vaughan, D., Anwyl, R. & Rowan, M. J. Adaptive changes in 5-HT$_{1A}$ receptor-mediated hippocampal inhibition in the alert rat produced by repeated 8-OH-DPAT treatment. *Brit. J. Pharmacol.* **112,** 1083–1089 (1994).

Acknowledgements. This research was supported by the Health Research Board of Ireland, the European Union DGXII and the Wellcome Trust.

Correspondence and requests for materials should be addressed to M.J.R. (e-mail:mrowan@mail.tcd.ie).

Impaired learning and LTP in mice expressing the carboxy terminus of the Alzheimer amyloid precursor protein

J. Nalbantoglu*†‡, G. Tirado-Santiago§, A. Lahsaïni‖, J. Poirier†¶, O. Goncalves‡, G. Verge‡, F. Momoli¶, S. A. Welner¶, G. Massicotte‖, J.-P. Julien*# & M. L. Shapiro§

Departments of Neurology & Neurosurgery, § Psychology, ¶ Psychiatry, † McGill Centre for Studies in Aging, McGill University, Montreal, Quebec H3A 2B4, Canada*

‡ Montreal Neurological Institute, Montreal, Quebec H3A 2B4, Canada

‖ Université du Québec à Trois-Rivières, Trois-Rivières, Quebec G9A 5H7, Canada

 # Centre for Neuroscience, Montreal General Hospital, Montreal, Quebec H3G 1A4, Canada

Proteolytic processing of amyloid precursor protein (APP) through an endosomal/lysosomal pathway generates carboxy-terminal polypeptides that contain an intact β-amyloid domain[1–3]. Cleavage by as-yet unidentified proteases releases the β-amyloid peptide in soluble form[4–6]. In Alzheimer's disease, aggregated β-amyloid is deposited in extracellular neuritic plaques.

Although most of the molecular mechanisms involving β-amyloid and APP in the aetiology of Alzheimer's disease are still unclear, changes in APP metabolism may be important in the pathogenesis of the disease. Here we show that transgenic mice expressing the amyloidogenic carboxy-terminal 104 amino acids of APP develop, with ageing, extracellular β-amyloid immunoreactivity, increased gliosis and microglial reactivity, as well as cell loss in the CA1 region of the hippocampus. Adult transgenic mice demonstrate spatial-learning deficits in the Morris water maze and in maintenance of long-term potentiation (LTP). Our results indicate that alterations in the processing of APP may have considerable physiological effects on synaptic plasticity.

Transgenic mice were produced by using a construct containing an APP complementary DNA fragment encoding amino acids 591 to 695, which spans the amyloid-forming portion and the carboxy terminus of the human amyloid precursor protein, cloned into the first exon of the human neurofilament *NF-L* gene and under the transcriptional control of the *NF-L* regulatory sequences[7] (Fig. 1a). Analysis by northern blotting showed that three out of seven transgenic lines had human amyloid-derived transcripts (~900 base pairs (bp)) in their brain tissue, expressed at levels comparable to the endogenous APP gene (Fig. 1b). Furthermore, expression of the transgene was restricted to nervous tissue and followed the pattern of expression of *NF-L* (ref. 7; data not shown). The presence of multiple copies of the transgene did not disrupt NF-L metabolism as there was no difference in the amount of NF-L transcript or protein expressed in transgenic and control mice (data not shown). In immunoprecipitation experiments using an anti-C-terminus antibody[8], brain homogenates prepared from transgenic mice had an increase of 30–50% in the levels of 12K polypeptide (relative molecular mass 12,000; Fig. 1c). Several smaller polypeptides that were immunoreactive with a polyclonal antibody against synthetic β-amyloid peptide[1] were detectable by western blotting (Fig. 1d): the pattern of bands obtained is similar to the five C-terminal APP fragments detected in human brain[1]. No 4K band was seen on immunoblots or in immunoprecipitates.

Immunohistochemical analysis of brain tissue from transgenic mice revealed that, with ageing, the extracellular immunoreactivity

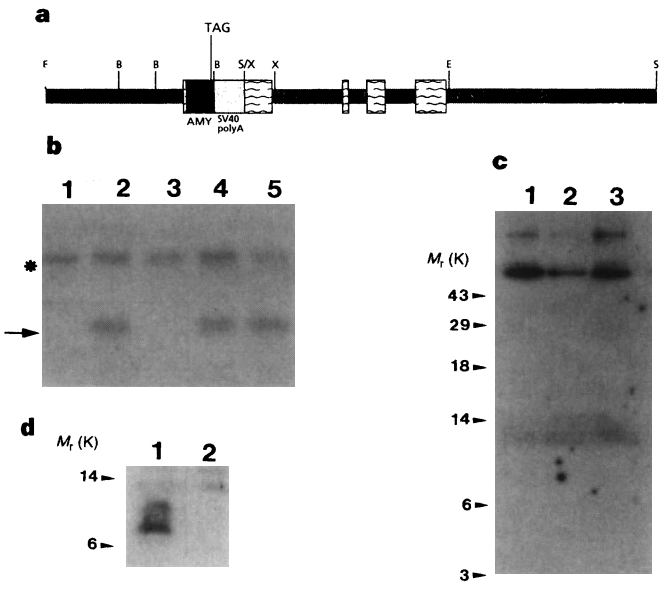

Figure 1 Expression of C-terminal amyloidogenic fragment of APP in transgenic brain. **a**, The construct: human *NF-L* gene upstream, intron and downstream genomic sequences are in grey; exon sequences are represented by white boxes. B, *Bam*HI; E, *Eco*RI; S, *Sal*I; X, *Xho*I; AMY, APP sequences; TAG, stop codon. **b**, Analysis of endogenous APP (asterisk) and transgenic mRNA (arrowed) levels in brain. Lane 1, control brain; lanes 2–5, transgenic brain. Note that no transgenic mRNA was detectable in lane 3 and the founder was not kept for further study. **c**, Immunoprecipitaiton of brain homogenates with an anti-C-terminus antibody[8]. Lane 1, control mouse brain; lanes 2, 3, transgenic mouse brain. **d**, Detection of amyloidogenic C-terminal fragments in brain homogenates (100 μg) of transgenic mice (lane 1) and control mice (lane 2) after electrophoresis on Tris/Tricine–16.5% polyacrylamide gel and immunoblotting with a polyclonal anti-amyloid antibody (SGY2347)[1].

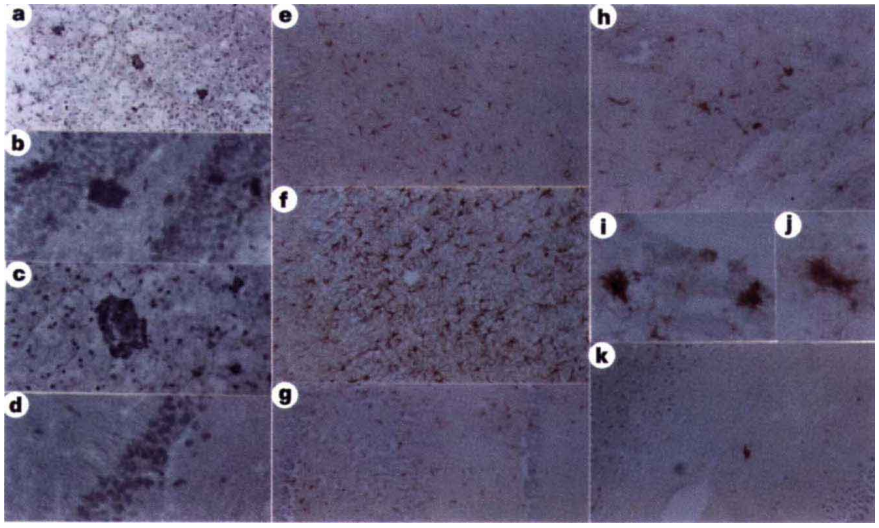

Figure 2 Immunohistochemical characterization of brain tissue from representative transgenic and age-matched control mice. Frozen sections were reacted with an anti-amyloid antibody (R1282) which revealed extracellular immunoreactivity in adult transgenic mouse cortex (**a**, **c**) and hippocampus (**b**); only intracellular reactivity was detected in hippocampus (**d**) of aged controls. Extensive gliosis was evident as anti-GFAP-positive astrocytes in the hippocampus of aged transgenics (**f**); adult transgenics (**e**) had more reactive astrocytes than aged controls (**g**) and young controls were devoid of immunoreactivity (not shown). Microglia that were detected with the anti-Mac-1 antibody in transgenic brain (**h**, **i**, **j**) were rare in control brain (**k**). Tissue was processed as described in Methods. Original magnifications: **a**, 150 ×; **b**–**d**, **i**, **j**, 600 ×; **e**–**h**, **k**, 300 ×.

for β-amyloid became more prevalent. The immunoreactivity was present as dense, compact structures in both cortex and hippocampus of only transgenic mice and was absent in controls (Fig. 2a–d). They were accompanied by generalized gliosis (Fig. 2e–g), which also increased with ageing: glial fibrillary acidic protein (GFAP)-positive reactive astrocytes, absent in controls, appeared as early as 4–5 months of age in hippocampal and cortical regions of the transgenic mice. Differences in microglial reactivity were evident in transgenic mice compared to age-matched controls (Fig. 2h–k). In our aged animals, cell counts in the CA1 region of the hippocampus[9] revealed a decrease in cell density of ~20% in transgenic animals ($0.295 \pm 0.06 \times 10^6$) compared to controls ($0.379 \pm 0.09 \times 10^6$) ($P < 0.001$). In this region, total neuron counts were also decreased in transgenic mice ($0.79 \pm 0.06 \times 10^4$) compared to control animals ($0.89 \pm 0.09 \times 10^4$) ($P < 0.007$).

To determine whether expression of the transgene in these animals imparted a phenotype, we characterized their behaviour in the Morris swim maze, which provides a sensitive assay for brain damage[10], particularly in the hippocampal or neocortical regions[11,12]. Mice are placed in a specific quadrant of a pool of

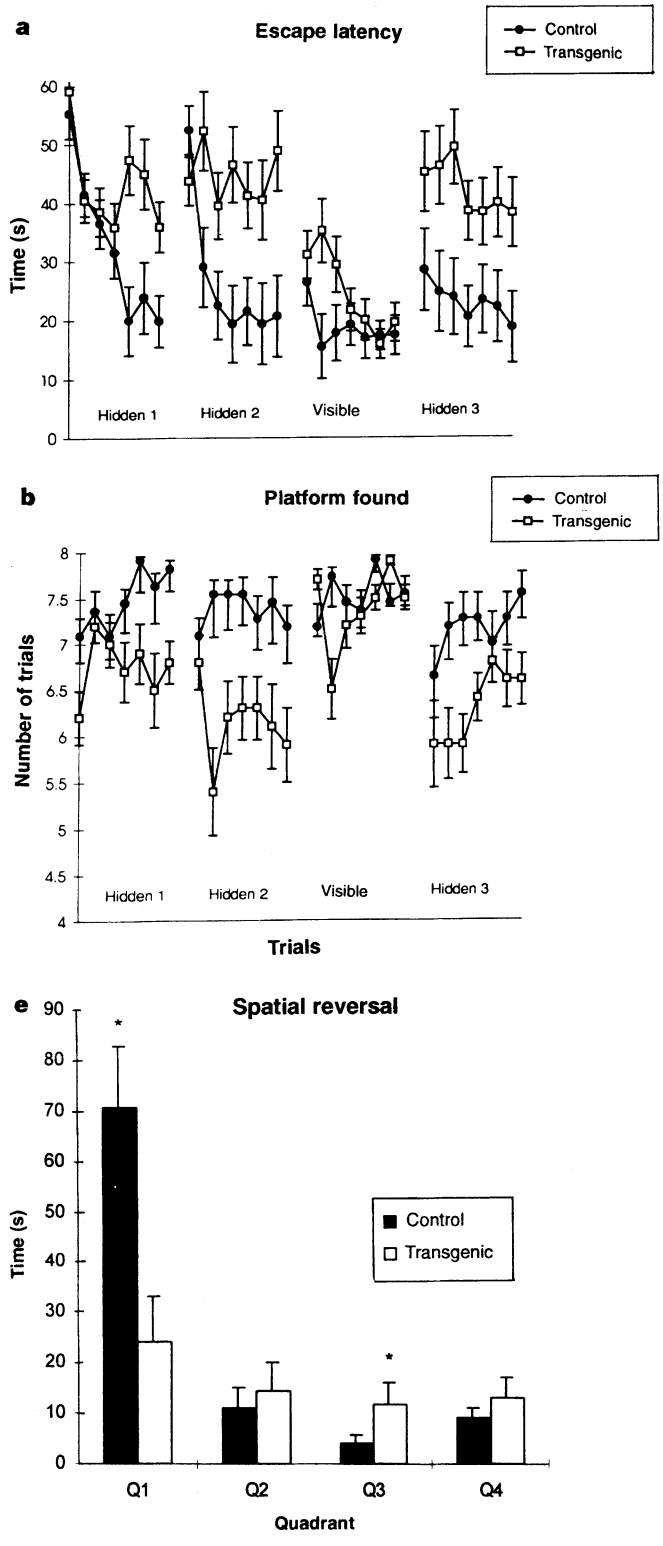

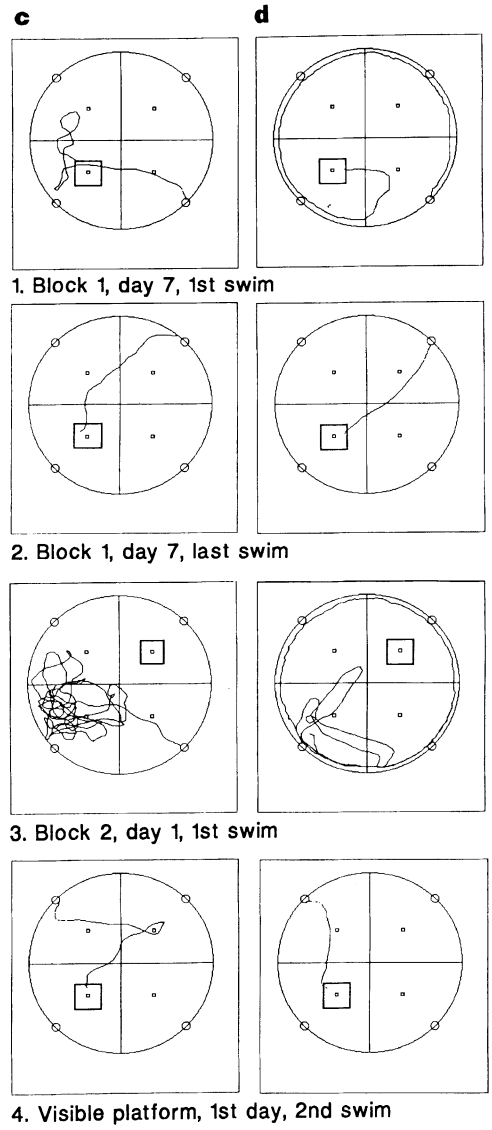

Figure 3 Performance of control (circles) and transgenic mice (squares) in the water maze was tested under four conditions, with the platform being hidden under the water in quadrants I, II and III of the tank (spatial learning), or made visible with a flag (cued learning). **a**, Escape latency. **b**, Number of trials in which mice found the platform during the 120-s trial. **c**, **d**, Examples of swim paths recorded during different stages of training for **c**, a control mouse and **d**, a transgenic mouse. Large squares show the platform locations, small squares indicate the quadrant centre, small circles the starting points, and lines the quadrants of the maze. **e**, The spatial probe trial was quantified by an ANOVA test comparing the total time spent in each of the four quadrants (Q1–4) of the maze. *$P < 0.05$.

opaque water and use spatial cues to escape to a hidden platform. Escape latency, the time required for the mice to swim to the platform, is an estimate of spatial learning and memory. To ensure that we used an unbiased measure of performance, the genetic background of the mice was coded and was unknown to the tester during the assessment. A trial began as soon as the mouse entered the water and ended as soon as it reached the platform or when 120 s had elapsed, whichever came first. Control adult mice learned to escape to the hidden platform in ~20 s after 5 days of testing in the first hidden platform condition (Fig. 3a and c2). The control mice performed equally well when the platform had to be found by visual guidance rather than spatial memory (Fig. 3a). In contrast, although transgenic mice improved on the hidden platform trials (Fig. 3a, d2), they were slower to find the hidden platform than control mice (3-way ANOVA (group, trial type, day) $F(18,342) = 2.84$, $P < 0.001$), and the impairment was significant in the first two tests of spatial learning (d.f.(1,19) = hidden 1, $F = 3.24$, $P < 0.05$; hidden 2, $F = 4.2$, $P < 0.05$, both 1-tailed) (Fig. 3a). In the visible platform trials, transgenic mice learned normally and no performance differences existed by the final 4 days of cued learning (visible, $F(1,19) = 0.14$, $P = 0.71$) (Fig. 3a, b). Furthermore, whereas the control mice typically found the platform within the allotted 120 s in every trial, the transgenic mice found the hidden platform within the allotted time significantly less frequently than the control mice during the last three trials in hidden 1 and hidden 2 ($F(1,19) \geq 3.0$, $P \leq 0.05$, 1-tailed), but they found the visible platform normally ($P = 0.99$) (Fig. 3b).There were no differences in swimming abilities as the transgenic mice swam faster but with less spatial accuracy than the controls; on average, transgenic mice swam longer distances, at a greater mean distance from the platform (data not shown). Transgenic mice did not differ from controls in general locomotor activity, as measured by interruptions of photocell beams in activity boxes equipped with photocell detectors (data not shown).

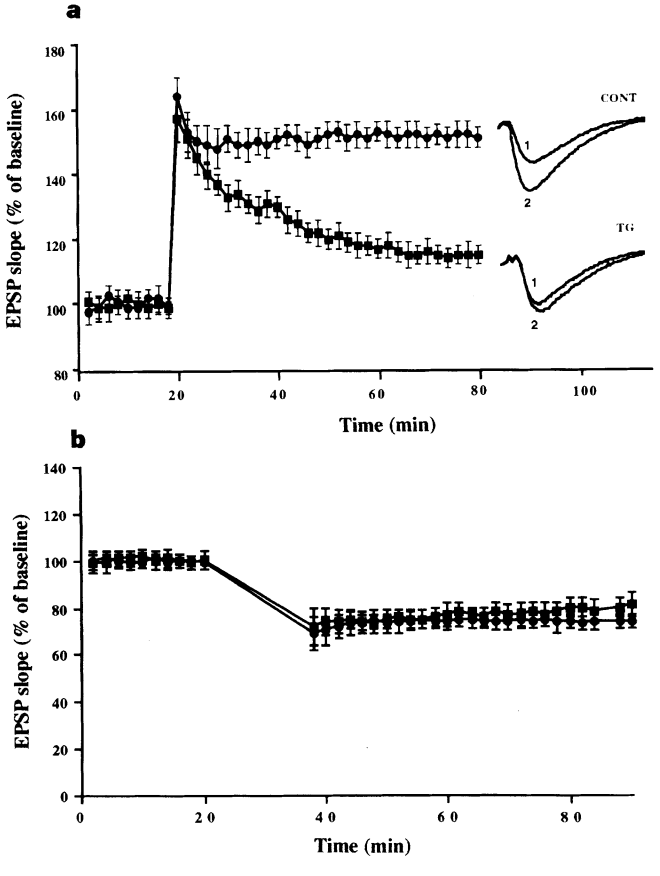

Figure 4 Reduced LTP magnitude (**a**) but normal LTD formation (**b**) in hippocampus of transgenic (squares) as compared to control mice (circles). **a**, LTP was measured in slices prepared from control ($n = 6$) and transgenic mice ($n = 6$). The initial slope of each excitatory postsynaptic potential (EPSP) evoked by electrical stimulation (every 30 s) in area CA1 of the hippocampus was calculated and the values of four successive responses were averaged. The baseline value represents the average of all the values obtained during the 20-min interval preceding theta burst stimulation. Data are expressed as percentage of the baseline value and each point represents the mean ± s.e.m. of 10 different experiments. Records were taken before (1) and 50 min after (2) theta burst stimulation. **b**, LTD was initiated by low-frequency stimulation (900 pulses at 1 Hz). Data are expressed as a percentage of the baseline value and each point represents the mean ± s.e.m. of 10 different experiments.

Examples of swim paths recorded during different stages of training for a control mouse and a transgenic mouse are shown in Fig. 3c, d. When the platform was moved to a different location (Fig. 3, c3 and d3), control mice swam persistently over the former platform location and thus took longer to find the platform in the reversal trial than the transgenic mice, whose more random swimming pattern meant that they intersected more quickly with the new platform location (Fig. 3a, hidden 2, first swim). The spatial bias of control mice (Fig. 3, c3) and the absence of such bias in transgenic mice (Fig. 3, d3) were confirmed statistically (interaction of quadrant by group: $F(3,57) = 10.8$, $P < 0.001$) (Fig. 3e). In contrast to transgenic mice, control mice spent more time in the first quadrant (Q1) than in the other quadrants (effect of quadrants: controls only, $F(3,30) = 26.8$, $P < 0.001$; transgenic only, $F(3,27) = 1.4$, $P < 0.27$). Control mice spent more time than the transgenic mice in Q1 ($F(1,19) = 10.3$, $P < 0.005$), whereas transgenic mice spent more time than the control mice in the opposite quadrant ($F(1,19) = 3.2$, $P < 0.05$ (1-tailed)) (Fig. 3e). Trials with the visible platform, in which transgenic mice swam directly towards the visible platform (Fig. 3, d4) indicated that the thigmotaxic behaviour shown early in spatial trials (Fig. 3, d1 and d3) was a consequence of impaired spatial learning, rather than a general alteration in behavioural strategy. These results indicate that the transgenic mice are selectively impaired in spatial learning but unimpaired in cued (visual discrimination) learning.

A model system for studying storage of memory and learning is through assay of synaptic plasticity, which can be induced by a short burst of high-frequency stimulation, a process known as long-term potentiation[13]. As shown in Fig. 4a, synaptic potentiation in CA1 was induced by theta burst stimulation (TBS) in hippocampal slices of control and transgenic mice. There was no significant modification in the degree of short-term potentiation in the first 2 min following TBS in transgenic mice (58 ± 6%; $n = 10$) compared to control mice (66 ± 7%, $n = 10$), but for the transgenic mice, there was a progressive decay of long-term potentiation (LTP) with time. A significant reduction in the magnitude of potentiation was found 10 min after TBS ($P < 0.05$, $n = 10$; Tukey test) and an even greater reduction after 50 min (52 ± 4% in control compared with 15 ± 4% in transgenics). There was a similar reduction in a second independent transgenic line (data not shown). The degree of paired-pulse facilitation measured in transgenic mice (40 ± 5%, $n = 5$) was not significantly modified when compared to that measured in control mice (45 ± 7%, $n = 7$). As paired-pulse facilitation is generally thought to be due to presynaptic enhancement of transmitter release, it may be assumed that presynaptic function is not altered in transgenic animals.

Long-term depression (LTD) is a second major form of activity-dependent synaptic plasticity[14]. LTD and LTP share many cellular substrates, but in LTD, low-frequency stimulation leads to a decrease in synaptic response. There were no differences in the degree of homosynaptic LTD between control and transgenic mice (Fig. 4b). These results demonstrate that whereas LTP maintenance is diminished in transgenic mice, normal LTD can be generated.

Table 1 Characteristics of transgenics expressing different isoforms/fragments of APP

Construct	Extracellular amyloid	Neuronal loss	Behavioural deficits		Electrophysiological alterations	Ref.
			Spatial	Cued		
APP (Val 717 → Phe)	+	ND	ND	ND	ND	28
APP_{751} (WT)	±	ND	+	−	ND	29
APP_{695} (Lys 670 → Asn; Met 671 → Leu)	+	ND	+	+*	ND	27
APP (C104)	+	+	+	−	+	This work

ND, not determined. WT, wild type.
* Transgenic mice were also impaired in the visible platform test.

To determine whether a reduction in NMDA (*N*-methyl-D-aspartate) receptor number and/or function might impair LTP in transgenic mice, the binding of 100 nM ^{3}H-glutamate was assayed. Autoradiography revealed no substantial changes in the amount of binding in various regions of the brain, including the CA1 stratum radiatum of the hippocampus (1.95 ± 0.15 pmol per mg protein in transgenic mice ($n = 4$) versus 2.07 ± 0.13 pmol mg^{-1} in controls ($n = 5$)). In addition, the NMDA-mediated response evoked in the presence of low Mg^{2+} and the AMPA (α-amino-3-hydroxy-5-methylisoxazole-4-proprionic acid) receptor antagonist DNQX (6,7-dinitroquinoxaline-2,3-dione) was normal in the transgenic mice (G.M., unpublished results). Thus, it is unlikely that a reduction in NMDA receptor function alone could account for the LTP deficit in transgenic mice.

In our transgenic mice, expression of a C-terminal amyloidogenic fragment led to tissue injury, with gliosis and microglial activation as well as extracellular amyloid immunoreactivity and hippocampal cell loss in the aged animals. There were marked behavioural and electrophysiological deficits in adults animals. Histological analysis and the selective changes in behaviour and electrophysiology, indicate that expression of human C-terminal APP in the brains of transgenic mice does not lead to massive and outright neuronal cell death as it does in neuronal cell lines transfected with constructs bearing this fragment[15,16]. Our results show that chronic overexpression of the amyloidogenic C-terminal fragment of APP is important physiologically. In Down's syndrome, duplication of the APP gene on chromosome 21 seems to be sufficient for amyloid deposition and subsequent development of Alzheimer-type neuropathology[17], so increased expression of the APP gene may alter the processing of the protein, producing more insoluble β-amyloid. *In vitro* studies with synthetic peptide have ascribed many neurotoxic effects to the aggregated form of β-amyloid[18–21], with the effects being mediated by reactive oxygen species[21], by alterations in intracellular calcium metabolism[19], or by interference with potassium[22] and calcium channels[23]. β-Amyloid can also activate microglia[24–26], generating free radicals which may damage neighbouring neural cells and initiate an inflammatory loop with the release of cytokines, locally increased levels of β-amyloid, and further activation of microglia. Varying degrees of extracellular amyloid immunoreactivity and some associated behavioural deficits (occurring as a function of genetic background[27]) have been reported in transgenic mice expressing different variants of APP (Table 1). Our discovery of early physiological perturbations that occur in transgenic mice expressing the amyloidogenic C-terminal fragment of human APP have important implications for the pathogenesis of Alzheimer's disease. □

Methods

Transgene construct. A *Bgl*II/*Pvu*II fragment (nucleotides 1,768 to 2,223) from the 3′-end of human APP cDNA[30] (encoding amino acid 591 to the termination codon) was cloned into the plasmid pSVL (Pharmacia). A *Sma*I/*Sal*I fragment containing the APP cDNA, as well as the SV40 late polyadenylation signal from pSVL, was cloned into a plasmid containing the entire human *NF-L* gene which had been digested by *Sma*I and partially by *Xho*I. Insertion of the APP clone was verified by sequencing. The entire 11.5-kb fragment was microinjected after removal of backbone plasmid sequences into fertilized oocytes from B6C3 F_1 mice.

Immunohistochemistry. Adult (8–10 months) or aged (18–22 months) mice were anaesthetized by intraperitoneal injection of chloral hydrate and perfused through the heart with a 4% solution of buffered paraformaldehyde. The brain was postfixed for 1 h with 4% buffered paraformaldehyde, and cryoprotected with 20% sucrose before freezing at − 50 °C and strorage at − 70 °C. Cryostat sections (15 μm thick) from transgenic and control animals were processed in parallel. Sections were treated with 88% formic acid for 5 min before assaying for anti-amyloid immunoreactivity with R1282 (diluted 1 : 1,000; provided by D. Selkoe) using a Vectastain ABC (Dimension Labs) kit for rabbit polyclonal antibodies. The signal from horseradish peroxidase was revealed with the enhanced diaminobenzidine substrate (Pierce). A polyclonal anti-cow GFAP antibody (Dako) that reacts strongly with the mouse GFAP was used at a dilution of 1 : 10,000 and the signal was revealed with the horseradish peroxidase substrate aminoethylcarbazol which produces an insoluble red product. Microglial reactivity was detected with anti-Mac-1 antibody (1 : 9) (prepared from the supernatant of the rat hybridoma M1/70.15.11.5.HL; obtained from the American Type Culture Collection). This antibody reacts against the I-subunit of Mac-1 antigen (complement receptor type 3) in mice and humans. An anti-rat secondary antibody was used to reveal specific staining with aminoethylcarbazol. Sections were counterstained with haematoxylin.

Cell counting. Neurons were counted on cryostat frozen 15-μm sections stained with cresyl violet prepared from aged transgenic ($n = 6$) and non-transgenic animals ($n = 12$). The entire CA1 region was delimited using a computer-assisted image analysis system (Biocom, France) which calculates areas automatically, and cells were counted for both hippocampi on each section ($n = 4$)[9]. Results were expressed as neuronal density (neurons per mm^3 ± s.d.). The transgenic population was considered to be homogeneous as the distribution of neuronal density was not different within the group (Kruskal–Wallis non-parametric analysis of variance test). Neuronal counts were obtained by serial sectioning of a segment spanning 250 μm of dorsal CA1. The Mann–Whitney non-parametric analysis of variance test was used to compare data obtained with transgenic and control mice.

Behavioural testing. Mice tested consisted of eight-month-old animals transgenic for the C-terminal fragment of APP ($n = 10$) or for the prokaryotic gene chloramphenicol acetyltransferase driven by the same human *NF-L* sequences ($n = 11$). Both lines of mice had been produced in the same transgenic mouse facility. The experimenter was blind to the genotype of the mice. The maze (170 cm in diameter and 70 cm of height) was lined with white coloured plastic and filled with a 45-cm column of opaque water (20 °C). For the testing phase, rectangular cues (22 × 28 cm) with differing geometric patterns were placed at 3 cm above the water at each of four locations between the quadrants. A video camera above the maze recorded the path swum by each mouse, and the path was stored by computer for further analysis. A training phase was administered to the mice to assess whether the animals could swim and whether they could climb onto the platform. Testing began the day after successfully determining that all test animals could swim to and climb onto the platform eight consecutive times. During the testing phase, each mouse was placed in the water facing the wall of the tank at one of the four starting points located at the centre of each quadrant. If a mouse did not climb onto the platform by the end of a maximum period of 120 s, it was placed onto the platform by hand. Each mouse was given eight swims a day. During testing carried out with the visible platform, the platform was moved to a new location

every day. A 3-way analysis of variance (ANOVA) compared the behaviour of the two groups across days and trial types.

Electrophysiological studies. Experiments were done on 450-μm-thick hippocampal slices prepared from control and transgenic mice. Slices were maintained at 35 °C in an artificial cerebrospinal fluid (ACSF) containing 124 mM NaCl, 5 mM KCl, 1.25 mM Na_2PO_4, 1.5 mM $MgCl_2$, 2.5 mM $CaCl_2$, 26 mM $NaHCO_3$ and 10 mM glucose pH 7.4. They were exposed to a humidified atmosphere of 95% O_2/5% CO_2 and perfused continuously at a flow rate of 1 ml min^{-1}. After a 1-hour equilibration, a glass recording electrode (1–5 mΩ) filled with 2 M NaCl was positioned in the stratum radiatum of area CA1 of the hippocampus to record population EPSPs evoked by a bipolar electrode activating fibres of the Schaffer commissural system. Bipolar stimulating electrodes were placed in the stratum radiatum of two independent pathways (Schaffer commissural pathways) converging on common postsynaptic target cells. The independence of each pathway was confirmed by the absence of heterosynaptic LTD or LTP in the pathway not receiving tetanic stimulation. After a 20-min baseline period, during which responses were recorded every 30 s, a low-frequency stimulation train of 1 Hz for 15 min (900 pulses) was applied to generate LTD; to increase presynaptic input activity, the duration of the stimulus was extended from 0.1 to 0.2 ms during low-frequency stimulation. LTP was produced by applying a high-frequency train consisting of high-frequency bursts (4 pulses, 100 Hz) repeated at 200 ms, the frequency of the hippocampal theta rhythm. The response to stimulation was quantified by calculating the initial slope of the resulting EPSP. The degree of paired-pulse facilitation was determined at an interpulse interval of 50 ms ($n = 5–7$) and data were expressed as a percentage increase in the amplitude of the second EPSP compared to the first.

Binding studies. Adjacent horizontal and coronal cryostat sections (14 μm) were preincubated for 60 min in 100 mM Tris-acetate buffer (pH 7.4) containing 100 μM EGTA at 0 °C. After a rapid wash in ice-cold Tris-acetate, sections were incubated with 100 nM ^{3}H-glutamate (51 Ci $mmol^{-1}$; NEN-Dupont) for 45 min at 4 °C in 50 mM Tris-acetate (pH 7.4), 50 μM EGTA, 5 μM AMPA, 1 μM kainic acid and 10 μM quisqualate to eliminate glutamate binding to non-NMDA sites, and 100 μM SITS (4-acetadino-4′-isothiocyanato-stilbene-2,2′-disulphonic acid) to block glutamate-uptake sites. Non-specific binding was defined as that measured in the presence of 1 mM glutamate. After washing, dried sections, as well as tritium standards (ARC), were exposed to tritium-sensitive film (Hyperfilm, Amersham) for 14 d. Optical densities of different brain regions were converted to radioactive units using the tritium standards after image analysis. ANOVA was followed by Scheffé post hoc test, with statistical significance set at $P < 0.05$.

Received 11 October 1996; accepted 9 April 1997.

1. Estus, S. *et al.* Potentially amyloidogenic carboxyl-terminal derivatives of the amyloid protein precursor. *Science* **255,** 726–728 (1992).
2. Haass, C., Koo, E. H., Mellon, A., Hung, A. Y. & Selkoe, D. J. Targeting of cell-surface β-amyloid precursor protein to lysosomes: alternative processing into amyloid-bearing fragments. *Nature* **357,** 500–502 (1992).
3. Golde, T. E., Estus, S., Younkin, L. H., Selkoe, D. J. & Younkin, S. G. Processing of the amyloid protein precursor to potentially amyloidogenic derivatives. *Science* **255,** 728–730 (1992).
4. Haass, C. *et al.* Amyloid β-peptide is produced by cultured cells during normal metabolism. *Nature* **359,** 322–325 (1992).
5. Shoji, M. *et al.* Production of the Alzheimer β-protein by normal proteolytic processing. *Science* **258,** 126–129 (1992).
6. Seubert, P. *et al.* Isolation and quantification of soluble Alzheimer's β-peptide from biological fluids. *Nature* **359,** 325–327 (1992).
7. Beaudet, L. *et al.* Intragenic regulatory elements contribute to transcriptional control of the neurofilament light gene. *Gene* **116,** 205–214 (1992).
8. LeBlanc, A. Increased production of 4 kDa amyloid β-peptide in serum deprived human primary neuron cultures: possible involvement of apoptosis. *J. Neurosci.* **15,** 7837–7846 (1995).
9. Meaney, M. J., Aitken, D. H., van Berkel, C., Bhatnagar, S. & Sapolsky, R. M. Effect of neonatal handling on age-related impairments associated with the hippocampus. *Science* **239,** 766–768 (1988).
10. Morris, R. G. M. Development of a water-maze procedure for studying spatial learning in the rat. *J. Neurosci. Meth.* **11,** 47–60 (1984).
11. Kolb, B., Sutherland, R. J. & Wishaw, I. Q. A comparison of the contributions of the frontal and parietal association cortex to spatial localization in rats. *Behav. Neurosci.* **97,** 13–27 (1983).
12. Skelton, R. W. & McNamara, R. K. Bilateral knife cuts to the perforant path disrupt spatial learning in the Morris water maze. *Hippocampus* **2,** 73–80 (1992).
13. Bliss, T. V. P. & Collingridge, G. L. A synaptic model of memory: long-term potentiation in the hippocampus. *Nature* **361,** 31–39 (1993).
14. Bear, M. F. & Malenka, R. C. Synaptic plasticity: LTP and LTD. *Curr. Opin. Neurobiol.* **4,** 389–399 (1994).
15. Yankner, B. A. *et al.* Neurotoxicity of a fragment of the amyloid precursor associated with Alzheimer's disease. *Science* **245,** 417–420 (1989).
16. Yoshikawa, K., Aizawa, T. & Hagashi, Y. Degeneration *in vitro* of post-mitotic neurons overexpressing the Alzheimer amyloid protein precursor. *Nature* **359,** 64–67 (1992).
17. Hyman, B. T. Down syndrome and Alzheimer disease. *Prog. Clin. Biol. Res.* **379,** 123–142 (1992).
18. Yankner, B. A., Duffy, L. K. & Kirschner, D. A. Neurotrophic and neurotoxic effects of amyloid β-protein: reversal by tachykinin neuropeptides. *Science* **250,** 279–282 (1990).
19. Mattson, M. P. *et al.* β-amyloid peptides destabilize calcium homeostasis and render human cortical neurons vulnerable to excitotoxicity. *J. Neurosci.* **12,** 376–389 (1992).
20. Loo, D. T. *et al.* Apoptosis is induced by β-amyloid in cultured central nervous system neurons. *Proc. Natl Acad. Sci. USA* **90,** 7951–7955 (1993).
21. Behl, C., Davis, J. B., Lesley, R. & Schubert, D. Hydrogen peroxide mediates amyloid β-protein toxicity. *Cell* **77,** 817–822 (1994).
22. Etcheberrigaray, R., Ito, E., Kim, C. S. & Alkin, D. L. Soluble β-amyloid induction of Alzheimer's phenotype of human fibroblast K^+ channels. *Science* **264,** 276–279 (1994).
23. Arispe, N., Rojas, J. & Pollard, H. B. Alzheimer disease amyloid β protein forms calcium channels in bilayer membranes: blockade by tromethamine and aluminum. *Proc. Natl Acad. Sci. USA* **90,** 567–571 (1993).
24. Meda, L. *et al.* Activation of microglial cells by β-amyloid protein and interferon-γ. *Nature* **374,** 647–650 (1995).
25. Yan, S. D. *et al.* RAGE and amyloid β-peptide. *Nature* **382,** 685–691 (1996).
26. El Khoury, J. *et al.* Scavenger receptor-mediated adhesion of microglia to β-amyloid fibrils. *Nature* **382,** 716–719 (1996).
27. Hsiao, K. *et al.* Correlative memory deficits, Aβ elevation and amyloid plaques in transgenic mice. *Science* **274,** 99–103 (1996).
28. Games, D. *et al.* Alzheimer-type neuropathology in transgenic mice expressing V717F β-amyloid precursor. *Nature* **373,** 523–526 (1995).
29. Quon, D. *et al.* Formation of β-amyloid protein deposits in brains of transgenic mice. *Nature* **352,** 239–241 (1991).
30. Kang, J. *et al.* The precursor of Alzheimer's disease amyloid A4 protein resembles a cell-surface receptor. *Nature* **325,** 733–736 (1987).

Acknowledgements. We thank A. LeBlanc, D. Selkoe and S. Younkin for antibodies, and Advanced Bioconcept Inc. for support. This work was funded by the MRC of Canada (J.N.), the Mental Health Network of Fonds de la recherche en santé du Québec (FRSQ) (J.N., J.P., S.W., G.M.) and NSERC (M.L.S.). J.N. and J.P. are research scholars of the FRSQ and J.-P.J. is a scientist of the MRC.

Correspondence and requests for materials should be addressed to J.N. (e-mail: josephine@rclvax.medcor.mcgill.ca).

Distinct ATP receptors on pain-sensing and stretch-sensing neurons

Sean P. Cook*, Lucy Vulchanova†, Kenneth M. Hargreaves†, Robert Elde† & Edwin W. McCleskey*

* *Vollum Institute L-474, Oregon Health Sciences University, 3181 SW Sam Jackson Park Road, Portland, Oregon 97201-3098, USA*
† *Department of Cell Biology and Neuroanatomy, University of Minnesota, Minneapolis, Minnesota 55455, USA*

The initial pain from tissue damage may result from the release of cytoplasmic components that act upon nociceptors, the sensors for pain. ATP was proposed to fill this role[1,2] because it elicits pain when applied intradermally[3] and may be the active compound in cytoplasmic fractions that cause pain[4]. Moreover, ATP opens ligand-gated ion channels (P2X receptors) in sensory neurons[5,6,7] and only sensory neurons express messenger RNA for the P2X3 receptor[8,9]. To test whether ATP contributes to nociception, we developed a tissue culture system that allows comparison of nociceptive (tooth-pulp afferent) and non-nociceptive (muscle-stretch receptor) rat sensory neurons. Low concentrations of ATP evoked action potentials and large inward currents in both types of neuron. Nociceptors had currents that were similar to those of heterologously expressed channels containing P2X3 subunits, and had P2X3 immunoreactivity in their sensory endings and cell bodies. Stretch receptors had currents that differed from those of P2X3 channels, and had no P2X3 immunoreactivity. These results support the theory that P2X3 receptors mediate a form of nociception, but also suggest non-nociceptive roles for ATP in sensory neurons.

In primary cultures of sensory neurons, nociceptors coexist with neurons that transduce other sensations. Although many *in vitro* techniques identify subpopulations of these neurons, no method identifies sensory modality[10,11]. The inability directly to compare neurons that mediate nociceptive and non-nociceptive sensations confounds investigation of the role of ATP in specific sensations